

**Realization of random-field Ising ferromagnetism in a molecular magnet**Bo Wen,<sup>1</sup> P. Subedi,<sup>2</sup> Lin Bo,<sup>1</sup> Y. Yeshurun,<sup>1,2,3</sup> M. P. Sarachik,<sup>1</sup> A. D. Kent,<sup>2</sup> A. J. Millis,<sup>4</sup>  
C. Lampropoulos,<sup>5</sup> and G. Christou<sup>5</sup><sup>1</sup>*Department of Physics, City College of New York, CUNY, New York, New York 10031, USA*<sup>2</sup>*Department of Physics, New York University, New York, New York 10003, USA*<sup>3</sup>*Department of Physics, Institute of Nanotechnology, Bar-Ilan University, Ramat-Gan 52900, Israel*<sup>4</sup>*Department of Physics, Columbia University, New York, New York 10027, USA*<sup>5</sup>*Department of Chemistry, University of Florida, Gainesville, Florida 32611, USA*

(Received 2 May 2010; published 8 July 2010)

The longitudinal magnetic susceptibility of single crystals of the molecular magnet Mn<sub>12</sub>-acetate obeys a Curie-Weiss law, indicating a transition to a ferromagnetic phase at  $\sim 0.9$  K. With increasing magnetic field applied transverse to the easy axis, a marked change is observed in the temperature dependence of the susceptibility, and the suppression of ferromagnetism is considerably more rapid than predicted by mean-field theory for an ordered single crystal. Our results can instead be fit by a Hamiltonian for a random-field Ising ferromagnet in a transverse magnetic field, where the randomness derives from the intrinsic distribution of locally tilted magnetic easy axes known to exist in Mn<sub>12</sub>-acetate crystals, suggesting that Mn<sub>12</sub>-acetate is a realization of the random-field Ising model in which the random field may be tuned by a field applied transverse to the easy axis.

DOI: [10.1103/PhysRevB.82.014406](https://doi.org/10.1103/PhysRevB.82.014406)

PACS number(s): 75.50.Xx, 64.70.Tg, 75.30.Kz, 75.50.Lk

**I. INTRODUCTION**

Interacting Ising spins that preferentially orient either “up” or “down” form a basis for understanding a broad range of complex natural phenomena. Long ranged order competes with thermal and quantum spin fluctuations and with the randomness which is present in any real material. A fundamental model used to study the interplay between these effects is the transverse field Ising model in a random magnetic field.<sup>1-3</sup> The essential feature of the random field is that it couples linearly to the order parameter, locally favoring one orientation over the other. Despite the interest in the physics of random-field models, there have been few experimental studies because of the difficulty of producing a magnetic field that varies randomly from site to site. The effect of random fields has been tested so far mainly in antiferromagnets following the observation of Fishman and Aharony<sup>4</sup> that in a site-diluted antiferromagnet a spatially uniform applied transverse magnetic field produces a random field which acts on the antiferromagnetic order parameter. The only ferromagnetic material found to date that shows characteristics of random fields is the rare earth dipolar ferromagnet LiHo<sub>x</sub>Y<sub>1-x</sub>F<sub>4</sub>.<sup>5</sup> In the undoped material ( $x=1$ ),  $T_C$  is found to decrease gradually with increasing applied transverse field,  $H_{\perp}$ , as  $(1-H_{\perp}^2)$ , consistent with mean-field theory (MFT). By contrast, dilution of the magnetic Ho ions with nonmagnetic Y ions reveals a fundamentally different behavior. In particular, the material with  $x=0.44$  exhibits a much stronger, approximately linear, decrease of  $T_C$  with  $H_{\perp}$ . This has been attributed to the fact that a transverse field applied to a site-diluted ferromagnet leads to a random longitudinal field.<sup>6</sup> However, several factors have made it difficult to obtain unambiguous results in the case of LiHo<sub>x</sub>Y<sub>1-x</sub>F<sub>4</sub>. The two most important are that dilution leads to randomness in the interactions themselves, thus changing the physics, and that the hyperfine fields are large and comparable to the dipole fields, further complicating the analysis.<sup>7,8</sup>

In this paper we report an experimental realization of a system with tunable random magnetic fields in single crystals of the prototypical molecular nanomagnet Mn<sub>12</sub>-acetate (henceforth abbreviated as Mn<sub>12</sub>-ac).<sup>9-11</sup> The hyperfine fields are relatively unimportant in this system and there is no intentional dilution of the lattice. The intermolecular interactions are predominantly dipolar in nature,<sup>12</sup> and Mn<sub>12</sub>-ac is thus a realization of a dipole-coupled Ising ferromagnet. The randomness arises from small tilts of the magnetic easy axis of individual molecules.<sup>13-19</sup> In the absence of an applied magnetic field the tilts have negligible effect on the magnetic properties. However, the tilts imply that a field applied transverse to the easy (Ising) axis has a nonvanishing projection along the local spin quantization axis, leading to a random longitudinal field of scale set by the applied transverse field. Mn<sub>12</sub>-ac and other single-molecule magnets may therefore serve as clean model systems for the study of random-field ferromagnetism where the random fields are controllable and considerably larger than typical hyperfine fields. This discovery promises to enable widespread and convenient experimental study of magnetism in a random field in a broad class of new materials.

**II. Mn<sub>12</sub>-ACETATE**

Mn<sub>12</sub>-ac [Mn<sub>12</sub>O<sub>12</sub>(O<sub>2</sub>CCH<sub>3</sub>)<sub>16</sub>(H<sub>2</sub>O)<sub>4</sub>]-2CH<sub>3</sub>CO<sub>2</sub>H-4H<sub>2</sub>O, the first-synthesized and best studied example of a single-molecule magnet, has been modeled as an Ising system. Each Mn<sub>12</sub>-ac molecule behaves as a nanomagnet with spin  $S=10$  with a strong uniaxial magnetic anisotropy, with Hamiltonian  $H_{mol} = -DS_z^2 - BS_z^4 + \dots$ , where  $D=0.548$  K,  $B=0.0012$  K and the ellipsis denotes additional small terms. The molecules crystallize in a body centered tetragonal lattice (with lattice constants  $a=b=1.7167$  nm,  $c=1.2254$  nm) and the distance between them is sufficiently large that the intercluster exchange is negligible compared to the intermo-

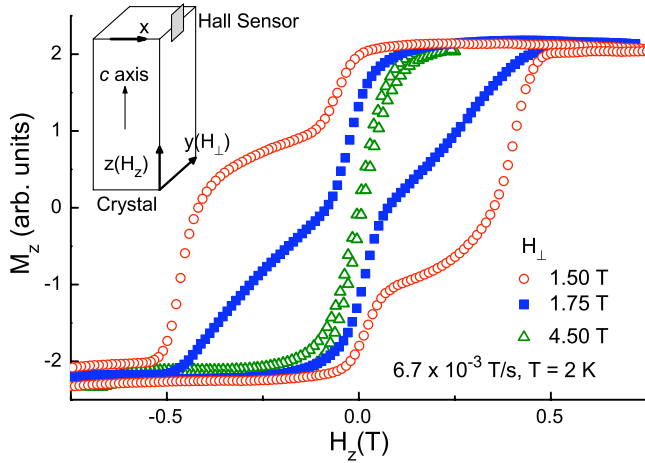


FIG. 1. (Color online) Longitudinal magnetization as a function of the longitudinal-field swept at  $6.7 \times 10^{-3}$  T/s for the indicated transverse magnetic fields at  $T=2.0$  K. Inset: schematic of the experiment setup, showing the relative positions of sample, Hall sensor and applied magnetic field.

lecular magnetic dipole interactions.<sup>12</sup> The strength of the intermolecular dipole interactions,  $E_{dip} = (g\mu_B)^2 S^2 / (a^2 c) \sim 0.08$  K, is one order of magnitude larger than intramolecular hyperfine interactions and leads to magnetic ordering with a Curie temperature of about 0.9 K in the absence of applied magnetic fields.<sup>20,21</sup>

### III. EXPERIMENT

#### A. Sample preparation and measurement techniques

The  $\text{Mn}_{12}\text{-ac}$  samples used in this study were synthesized as described by Lis.<sup>22</sup> A miniature Hall sensor (active area  $50 \times 50 \mu\text{m}^2$ ) was used to measure the longitudinal magnetization,  $M_z$ , along the easy direction ( $c$ -axis) of the crystal. Measurements were performed on two  $\text{Mn}_{12}\text{-ac}$  single crystals (sample A, dimensions  $\sim 0.4 \times 0.4 \times 2.17 \text{ mm}^3$  and sample B, dimensions  $\sim 0.4 \times 0.4 \times 2.4 \text{ mm}^3$ ). Data are shown for sample B; sample A displays the same qualitative behavior but has a lower transition temperature of 0.5 K in zero transverse field.<sup>23</sup> The sensor was placed near the edge of the sample, where the measured  $B_x$  is a linear function of  $M_z$ . Care was taken to align the sample and the Hall bar (placed in the  $y$ - $z$  plane) relative to each other and relative to the applied magnet fields. Measurements were taken between 0.7 and 5.5 K in a  $^3\text{He}$  refrigerator with a three-dimensional (3D) superconducting vector magnet. A longitudinal field,  $H_z$ , was swept along the sample's easy axis at rates between  $1 \times 10^{-5}$  and  $6.7 \times 10^{-4}$  T/s, in the presence of a constant transverse field  $H_\perp$  (up to 5 T) applied in the  $y$  direction (see inset of Fig. 1).

#### B. Measurement of the equilibrium susceptibility

Below a blocking temperature  $T_B \sim 3$  K in the absence of applied transverse field, the longitudinal magnetization of  $\text{Mn}_{12}\text{-ac}$  exhibits hysteresis due to slow spin reversal and steps in the magnetic hysteresis loops due to quantum tun-

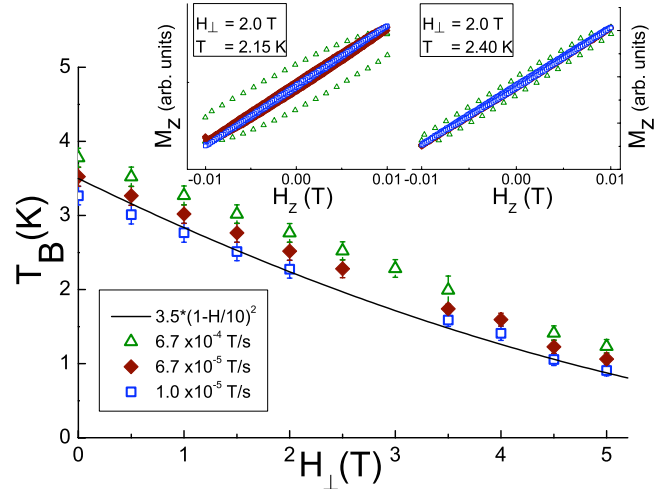


FIG. 2. (Color online) Determination of the blocking temperature. Insets: Magnetization as a function of the longitudinal-field swept at the indicated rates for  $H_\perp = 2$  T at  $T = 2.15$  K and  $T = 2.40$  K. Main panel: Blocking temperatures for three longitudinal-field sweep rates as a function of  $H_\perp$ .

neling between opposite spin projections.<sup>10</sup> A transverse field,  $H_\perp$ , applied perpendicular to the crystal  $z$  axis increases the spin-reversal rate, thereby reducing  $T_B$ .<sup>24,25</sup> The blocking temperature depends also on the longitudinal-field sweep rate,  $\alpha = \partial H_z / \partial t$ . Slow spin relaxation and hysteresis preclude measurements of equilibrium properties at the low temperatures at which magnetic ordering occurs. Our approach is, therefore, to deduce the nature of the magnetic interactions from measurements of the magnetic susceptibility at temperatures above the blocking temperature.

In order to establish the range of experimental conditions in which it is possible to measure the equilibrium susceptibility we first determined  $T_B$  as a function of transverse field and longitudinal-field sweep rate. The magnetization of  $\text{Mn}_{12}\text{-ac}$  is shown in Fig. 1 for different transverse magnetic fields at  $T=2$  K and a longitudinal-field sweep rate of  $6.7 \times 10^{-3}$  T/s. The magnetization exhibits hysteresis and the steps characteristic of resonant tunneling.<sup>10</sup> The hysteresis can be eliminated by applying a transverse field or by sweeping the longitudinal field sufficiently slowly. The effect of transverse field is clearly demonstrated in Fig. 1: as the transverse field increases, relaxation processes are accelerated, the width of the hysteresis loops decreases, the steps disappear, and equilibrium is ultimately reached so that the magnetization exhibits reversible behavior.

The effect of reducing the sweep rate is demonstrated in the two insets of Fig. 2 which show the hysteresis loops obtained for three different longitudinal magnetic field sweep rates in a narrow range  $\pm 0.01$  T about  $H_z=0$ , measured in the presence of a constant transverse field  $H_\perp = 2$  T at  $T = 2.15$  K and  $T = 2.40$  K. The point  $H_z=0$  T was determined by symmetry from full magnetization curves taken between  $-0.75$  T and  $0.75$  T (see Fig. 1). In each case, hysteresis is observed at the faster sweep rate indicating that the system is below the blocking temperature; at the slower sweep rate the hysteresis loop is closed, indicating the system is above the blocking temperature and equilibrium is reached. From these

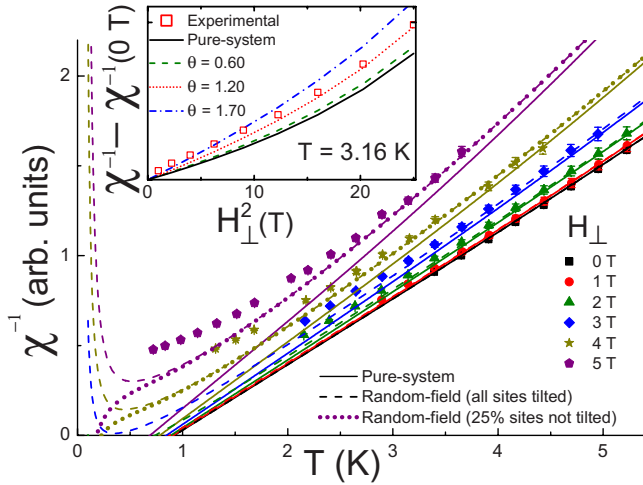


FIG. 3. (Color online) Temperature and field dependence of the inverse susceptibility of  $\text{Mn}_{12}\text{-ac}$ . Main panel: filled symbols denote the inverse susceptibility of a single crystal of  $\text{Mn}_{12}\text{-ac}$  as a function of temperature in different transverse fields  $H_{\perp}$  as labeled. The solid lines are the result of mean-field calculations for a hypothetical system with no tilts. The dashed lines are obtained from mean-field calculations incorporating the effects of random tilt angles, as discussed in Sec. IV B of the main text with root mean square tilt angle  $1.2^{\circ}$ . The dotted lines present theoretical results for a different distribution with the same mean square tilt angle but in which 25% of the sites are not tilted. Inset: Symbols represent the difference  $[\chi^{-1}(H_{\perp}) - \chi^{-1}(H_{\perp}=0)]$  versus  $H_{\perp}^2$ . The dashed, dotted and dash-dotted lines are calculated using the model of Sec. IV B but with different root mean square tilt angles as indicated. The solid line displays results for the pure case.

and similar data we deduce the field dependence of  $T_B$ , as summarized in Fig. 2 for three different longitudinal-field sweep rates. The applied transverse field  $H_{\perp}$  accelerates the relaxation of the magnetization toward equilibrium, lowering the blocking temperature,  $T_B$ , as expected based on the  $\text{Mn}_{12}\text{-ac}$  spin Hamiltonian. Note that a reduction in  $T_B$  is also expected from a classical model of single domain uniaxial nanomagnets—the classical version of  $\text{Mn}_{12}\text{-ac}$ —where  $T_B = (1-h)^2$ ,  $h = H/H_A$ ,  $H$  is the externally applied transverse field and  $H_A$  is the anisotropy field ( $H_A = 2DS/g\mu_B \approx 10$  T).<sup>26</sup> The solid line in Fig. 2 is a fit of the measured  $T_B$  to the predicted quadratic dependence on field.

### C. Longitudinal susceptibility

Figure 3 shows the main experimental results presented in this paper: the measured equilibrium longitudinal susceptibility of a  $\text{Mn}_{12}\text{-ac}$  single crystal versus temperature and applied transverse field. As noted, these measurements were performed at temperatures above  $T_B(H_{\perp}, \alpha)$  (see, Fig. 2). The longitudinal magnetic susceptibility,  $\chi = \partial M_z / \partial H_z|_{H_{\perp}=0}$ , was deduced from the slope of the reversible  $M_z$  versus  $H_z$  at  $H_z=0$ . The solid symbols in Fig. 3 show the inverse of the longitudinal susceptibility as a function of temperature for transverse fields between zero and 5 T. For zero transverse field  $\chi^{-1}$  obeys the Curie-Weiss law expected from mean-field theory (MFT),  $\chi^{-1} \sim (T - T_{CW})$ . The solid black line is a

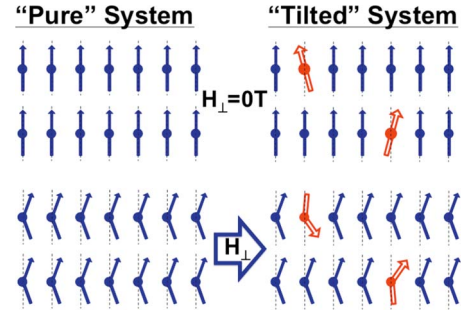


FIG. 4. (Color online) Effect of easy axis tilts on the transition temperature. In zero field a perfectly ordered crystal and a crystal in which there are easy axis tilts (e.g., the double-line red spins) will order at nearly the same temperature (the small tilts do not greatly modify the interaction between spins, which depends on the longitudinal component of the magnetic moment). In an applied transverse field, the spins of misaligned molecules experience a field along their Ising axis. When this field is comparable to the exchange field these spins are frozen (double-line red spins) and do not order. This leads to an effective dilution of the spins, a decrease in the susceptibility and a reduction in the transition temperature. It also increases the random field on the other sites in the crystal.

fit of the data in zero transverse field to Curie-Weiss theory; the intercept  $T_{CW} \sim 0.9$  K implies a transition at this temperature from paramagnetism (PM) to ferromagnetism (FM), consistent with the result of Luis *et al.*<sup>11</sup> As  $H_{\perp}$  is increased from zero, there is a systematic increase in the inverse susceptibility. The application of a transverse field is expected to increase  $\chi^{-1}$  and decrease the ordering temperature.<sup>27</sup> However, as the field increases the data exhibits progressively larger deviations from the straight-line behavior found at  $H_{\perp}=0$ .

## IV. THEORY

### A. Randomness in $\text{Mn}_{12}\text{-ac}$

While the susceptibility of  $\text{Mn}_{12}\text{-ac}$  in small transverse fields is well described by mean-field theory using a Hamiltonian for a well-ordered “pure” system, it is clear that this model fails to describe the data obtained in the presence of a large transverse field, indicating the presence of physics not included in the pure-system calculation. We argue that the additional physics is a random-field effect arising from structural disorder in the  $\text{Mn}_{12}\text{-ac}$  crystal.<sup>13–19</sup> In particular, different isomers of the host acetate material have been shown<sup>12</sup> to cause the spin quantization axis of some of the  $\text{Mn}_{12}\text{-ac}$  molecules to tilt away from the crystal  $z$ -axis by a small monomer-dependent angle  $\theta$ . As illustrated schematically in Fig. 4, on sites with a nonzero tilt angle a magnetic field applied transverse to the crystal  $z$  axis has a component directed along the spin quantization axis; these longitudinal components are randomly distributed, and their magnitude is controlled by the size of the externally applied transverse field.

### B. Theoretical model

In this section we introduce a slightly refined version of a theoretical model of  $\text{Mn}_{12}\text{-ac}$  introduced by Millis *et al.*<sup>21</sup>

The model uses mean-field theory (MFT) to calculate the inverse magnetic susceptibility as  $\chi^{-1} = \chi_{mol}^{-1} - J$ , with  $\chi_{mol}^{-1}$  obtained from an exact solution of the single-molecule Hamiltonian  $H_{mol}$ . For the intersite interaction we use the dipolar form generally accepted for  $Mn_{12}$ ,<sup>12</sup> specialized to the lattice appropriate to  $Mn_{12}$  (see Millis *et al.*<sup>21</sup>). A model with short ranged interactions would exhibit very similar physics. The single-molecule Hamiltonian is the sum of two terms, namely, a term that is the same for every  $Mn_{12}$ -ac and a random-field term which varies from site to site:  $H_{mol} = H_{mol}^0 + H_{mol}^{ran,i}$ . The term that is the same for every site is

$$H_{mol}^0 = -DS_z^2 - BS_z^4 + C(S_+^4 + S_-^4) + g\mu_B \vec{H}_\perp \cdot \vec{S}_\perp. \quad (1)$$

Here  $S_z, \vec{S}_\perp = (S_x, S_y, 0)$  and  $S_\pm$  are matrices from the  $S=10$  representation of  $SU(2)$  and  $D=0.548$  K,  $B=0.0012$  K,  $C=1.44 \times 10^{-5}$  K and we used  $g\mu_B=1.34$  K/T. Reference 21 employed a simplified version of Eq. (1) with  $B=C=0$  and  $D$  renormalized to reproduce the ground state tunnel splitting. We find that this commonly-used approximation is insufficiently accurate for our purposes: it leads to errors in the field dependence of the third and fourth levels of the  $S=10$  manifold which lead to errors in  $\chi_{mol}$  for  $H \gtrsim 4$  T and  $T \gtrsim 3$  K. The differences in  $H_{mol}$  are the source of the minor differences between the results presented here and those of Ref. 21. We find that  $C$  may be set to zero or doubled without changing the results.

The site-dependent term  $H_{mol}^{ran,i}$  arises from isomer effects in the host acetate molecule which lead to a misorientation of the  $Mn_{12}$ -ac spin-quantization (spin- $z$ ) axis with respect to the crystallographic  $z$  axis.<sup>19</sup> The misorientation is characterized by a small polar tilt  $\theta$  and an azimuthal angle  $\phi$  which we measure with respect to the direction  $\phi_H$  defined by the transverse field. Linearizing in  $\theta$  we obtain

$$H_{mol}^{ran,i} = \theta_i \cos(\phi_i + \phi_H) g\mu_B H_\perp S_z + E_i(S_x^2 - S_y^2). \quad (2)$$

We use the monomer distribution proposed by Park<sup>19</sup> which involves twelve inequivalent sites, each of which has its own specific tilt angle. We assume the sites are randomly distributed through the crystal except that (i) we treat the mean value of the angle as an adjustable parameter (in the theoretical calculations of Park<sup>19</sup> it is found to be about  $0.4^\circ$ ) and (ii) on the sites that Park argues have no tilts we take  $\theta$  to be 20% of its value on the tilted sites, reflecting our assumption of residual disorder. We note, however, that calculations in which  $\theta$  is set to zero in the relevant sites do not affect the data in the accessible temperature range. In the model proposed by Park both the average of  $\cos(\phi_i + \phi_H)$  and of  $E_i$  vanish. While we include the  $E$  term in our calculation with the typical value 0.008 K proposed by Park, we have verified that setting it to zero or tripling it does not change the results.

$H_{mol}^{ran,i}$  is a random function characterized by a distribution. For temperatures greater than about 2 K the only feature which is important is the mean square amplitude of the tilt angle

$$\theta_0 = \sqrt{\sum_i \theta_i^2}, \quad (3)$$

changing the form of the distribution but keeping  $\theta_0$  fixed leaves the results invariant. For lower temperatures, specific properties of the distribution become important, in particular the fraction of sites with vanishing random field (see dashed and dotted lines in Fig. 3 for  $T < 1$  K). In the Park model the angles  $\phi_i = n\pi/4$  with  $n=0, 1, 2, \dots, 7$  and the fraction of sites with very small random field may be controlled by varying  $\phi_H$ .

## V. THEORETICAL RESULTS AND COMPARISON TO DATA

The solid lines shown in Fig. 3 are the result of calculations for the pure system without randomness. As  $H_\perp$  is increased, the slope of the calculated traces increases, reflecting spin canting induced by the magnetic field. Also, due to the increase in quantum tunneling, the estimated ferromagnetic transition temperature (the extrapolated value where  $\chi^{-1}$  vanishes) decreases and the calculated traces develop a weak curvature at low temperatures. The pure-system calculation and the data agree well only at small transverse fields.

The dashed lines in Fig. 3 show the results of calculations that include the randomness associated with isomer tilts. Here we have assumed that all the sites have a tilt and the mean square tilt angle is  $1.2^\circ$ , larger than the  $0.4^\circ$  calculated by Park *et al.*<sup>12</sup> but in good accord with the values determined using EPR (Ref. 17) (which finds tilts up to  $1.7^\circ$ ). Although not in complete agreement with the data, the theory with randomness accounts for all the major features of the observed  $\chi^{-1}(T)$  in transverse fields.

The inset of Fig. 3 compares the measured and calculated field dependence of  $\chi^{-1}$  at a fixed temperature (3.16 K). The quadratic field dependence at low fields follows from general principles. The magnitude is seen to be inconsistent with the pure-system calculation (solid line) and consistent with the random-field calculation (dotted line), further supporting our proposal. The dotted line was calculated for a mean tilt angle of  $1.2^\circ$ . The dashed and dash-dotted lines, calculated for  $0.6^\circ$  and  $1.7^\circ$ , define the range of mean tilt angles that are consistent with the experimental data. We therefore conclude that MFT with randomness included accounts also for the field dependence of  $\chi^{-1}$ .

It is important to note that in the experimentally accessible temperature range the results are insensitive to the details of the distribution, depending only on the mean square tilt angle. This is demonstrated by the dashed and dotted lines in Fig. 3. These show calculations of  $\chi^{-1}(T)$  for 4 and 5 T obtained using a different distribution of the random field with the same mean square tilt angle of  $1.2^\circ$  as above, but with 25% of the sites not tilted, and correspondingly larger tilts on the remaining sites. The dashed and dotted lines overlap in most of the temperature range. However, as is clear from the figure, the behavior of  $\chi^{-1}(T)$  at lower temperatures does depend on the detailed distribution of tilts;  $\chi^{-1}$  approaches zero (i.e.,  $\chi$  diverges) when the distribution includes spins that are not tilted. This conclusion can be ex-

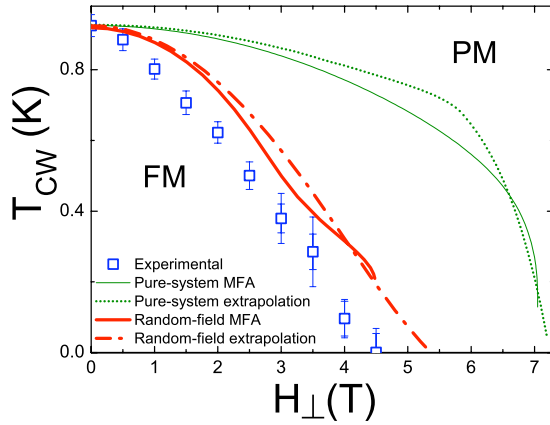


FIG. 5. (Color online) The Curie-Weiss and the ferromagnetic transition temperatures as a function of transverse field. The intercepts  $T_{CW}$  (squares) are obtained from the straight-line portion of the data curves in Fig. 3. The dotted and dash-dotted lines are mean-field  $T_{CW}$  results for the pure and random case, respectively. The light and heavy solid lines are mean-field transition temperatures,  $T_C$ , calculated for the pure and random case, respectively. In the random case at higher field, the detailed structure depends on the specific details of the distribution of random fields. Here we plot  $T_C$  using the distribution obtained by Park<sup>19</sup> where the parameters ( $\theta=1.2^\circ$  and  $\phi=0$ ) are the same as those used to fit the data in Fig. 3, and residual randomness is introduced as described in the text. For this assumed distribution and these parameters,  $T_C$  drops discontinuously to zero at 4.5 T.

perimentally tested, as the isomer distribution may be changed within this model by rotating the applied field in the plane perpendicular to the mean quantization axis.<sup>12,21</sup>

The effect of transverse field can be understood as follows. With or without randomness, a transverse field leads to a canting of the spins away from the  $z$  axis, as illustrated in Fig. 4, and to enhanced quantum fluctuations of the spin. Since the intermolecular dipole interaction is associated with the  $z$  component of spin, the dipole interaction strength is reduced in a transverse field. However, a transverse field much smaller than the anisotropy field  $H_A \approx 10$  T produces very little spin canting ( $\tan \theta_c = H_\perp / H_A$ ) and a negligible change in the interaction strength. Hence, for fields below about 3 T the susceptibility and the ordering temperature are virtually unchanged in the system without randomness. The FM order is very strongly suppressed only when the quantum fluctuations become important (when the tunnel splitting,  $\Delta$ , of the lowest spin states is comparable to the intermolecular dipole interactions, which occurs at  $\sim 7$  T for  $\text{Mn}_{12}\text{-ac}$ <sup>20,21</sup>). However, in the presence of the tilt disorder described above, for transverse fields that establish longitudinal-field components along the easy axis of tilted molecule comparable in magnitude to the intermolecular dipole field (approximately 50 mT,<sup>28</sup> corresponding to 3 T for a tilt angle of  $1^\circ$ ), the tilted spins can no longer participate in the FM order and there is an effective dilution of the spins which causes a rapid reduction of the susceptibility and of the ordering temperature.<sup>21</sup>

Figure 5 shows approximate values of the intercept  $T_{CW}$  (squares) obtained from fitting the high-temperature region

of the experimental curves shown in Fig. 3 to the Curie-Weiss law. The fit does not include data for which  $\chi^{-1} > 0.2$ , as the measured susceptibility exhibits a systematic background that reaches above 10% at values of  $\chi=0.5$ . Data at high transverse field and low temperatures were also ignored (the upturns in Fig. 3); in this region the tunnel splitting becomes larger than  $kT$  and, consequently, the susceptibility reflects the quantum state rather than being determined by the temperature. At small values of the transverse field the intercepts  $T_{CW}$  derived from extrapolation of the high-temperature data provides a reasonably reliable estimate for the mean-field transition temperature, but the extrapolations are less reliable as the transverse field is increased. Yet, the conclusion from Fig. 5 is clear: the application of transverse field leads to a strong, approximately linear reduction in  $T_{CW}$ . To estimate the reliability of the extrapolation and the significance of the strong reduction in  $T_{CW}$  we applied the same extrapolation procedure to the theoretical  $\chi^{-1}$  curves for the “pure” and random case (solid and dashed lines in Fig. 3, respectively); the calculated intercepts are shown in Fig. 5 by the dotted and dash-dotted lines, respectively. We also used the theoretical model to calculate the mean-field paramagnetic-ferromagnetic transition temperature,  $T_C$ , i.e., the temperature where  $\chi$  diverges ( $\chi^{-1}=0$ ). The calculated values of  $T_C$  for the pure and random cases are denoted in Fig. 5 by the solid dotted and dash-dotted lines, respectively. At low transverse fields (below 3 T), the calculated  $T_{CW}$  and the calculated ferromagnetic transition temperature  $T_C$  differ by less than 5%.

## VI. CONCLUSIONS

Based on measurements of magnetic susceptibility and magnetization, we report that the prototypical single-molecule magnet  $\text{Mn}_{12}\text{-ac}$  is a new archetype of random-field Ising ferromagnetism in transverse field. In this system, although the intrinsic randomness in the interaction is small, it is sufficient for an externally applied transverse magnetic field to generate a significant random field in the longitudinal direction. In addition to canting the spins, the transverse field reduces  $T_{CW}$  in two ways: (1) it introduces channels for quantum relaxation for each of the molecules, thereby inducing spin disorder, and (2) it induces fluctuations in the longitudinal field that are comparable with the intrinsic dipolar interactions themselves, thereby further depressing the ordering temperature. These factors give rise to a dependence of  $T_{CW}$  on  $H_\perp$  that is inconsistent with that expected from mean-field theory for a “pure” well-ordered system. We conclude that the rapid decrease of  $T_{CW}$  with increasing transverse field, as well as our ability to fit the susceptibility with a model that includes randomness, are strong evidence that  $\text{Mn}_{12}\text{-ac}$  is a particularly clean realization of random-field Ising ferromagnetism in a new class of materials.

## ACKNOWLEDGMENTS

We thank G. de Loubens and S. McHugh for valuable help during the initial phases of the experiment and Zhonghua Zhao for technical assistance. We acknowledge illumi-

nating discussions with E. Chudnovsky, J. R. Friedman, D. Garanin, A. Mitra, and M. Schechter. Support for G.C. was provided by NSF under Grant No. CHE-0910472; A.D.K. acknowledges support by NSF Grant No. NSF-DMR-0506946 and ARO Grant No. W911NF-08-1-0364; A.J.M.

acknowledges support of NSF-DMR-0705847; M.P.S. acknowledges support from Grant No. NSF-DMR-0451605; Y.Y. acknowledges support of the Deutsche Forschungsgemeinschaft through a Deutsch-Israelische Projektkooperation (DIP).

- 
- <sup>1</sup>Y. Imry and S.-k. Ma, *Phys. Rev. Lett.* **35**, 1399 (1975).  
<sup>2</sup>Y. Imry and M. Wortis, *Phys. Rev. B* **19**, 3580 (1979).  
<sup>3</sup>D. Belanger and A. Young, *J. Magn. Magn. Mater.* **100**, 272 (1991).  
<sup>4</sup>S. Fishman and A. Aharony, *J. Phys. C* **12**, L729 (1979).  
<sup>5</sup>D. M. Silevitch, D. Bitko, J. Brooke, S. Ghosh, G. Aeppli, and T. F. Rosenbaum, *Nature (London)* **448**, 567 (2007).  
<sup>6</sup>M. Schechter, *Phys. Rev. B* **77**, 020401 (2008).  
<sup>7</sup>R. Giraud, A. M. Tkachuk, and B. Barbara, *Phys. Rev. Lett.* **91**, 257204 (2003).  
<sup>8</sup>M. Schechter and P. C. E. Stamp, *Phys. Rev. Lett.* **95**, 267208 (2005).  
<sup>9</sup>D. Gatteschi, R. Sessoli, and J. Villain, *Molecular Nanomagnets* (Oxford University Press, Oxford, 2006).  
<sup>10</sup>J. R. Friedman, M. P. Sarachik, J. Tejada, and R. Ziolo, *Phys. Rev. Lett.* **76**, 3830 (1996).  
<sup>11</sup>F. Luis, J. Campo, J. Gómez, G. J. McIntyre, J. Luzón, and D. Ruiz-Molina, *Phys. Rev. Lett.* **95**, 227202 (2005).  
<sup>12</sup>K. Park, M. A. Novotny, N. S. Dalal, S. Hill, and P. A. Rikvold, *Phys. Rev. B* **66**, 144409 (2002).  
<sup>13</sup>A. Cornia, A. C. Fabretti, R. Sessoli, L. Sorace, D. Gatteschi, A.-L. Barra, C. Daugebonne, and T. Roisnel, *Acta Crystallogr., Sect. C: Cryst. Struct. Commun.* **58**, m371 (2002).  
<sup>14</sup>A. Cornia, R. Sessoli, L. Sorace, D. Gatteschi, A. L. Barra, and C. Daugebonne, *Phys. Rev. Lett.* **89**, 257201 (2002).  
<sup>15</sup>E. del Barco, A. D. Kent, E. M. Rumberger, D. N. Hendrickson, and G. Christou, *Phys. Rev. Lett.* **91**, 047203 (2003).  
<sup>16</sup>S. Hill, R. S. Edwards, S. I. Jones, N. S. Dalal, and J. M. North, *Phys. Rev. Lett.* **90**, 217204 (2003).  
<sup>17</sup>S. Takahashi, R. S. Edwards, J. M. North, S. Hill, and N. S. Dalal, *Phys. Rev. B* **70**, 094429 (2004).  
<sup>18</sup>E. del Barco, A. D. Kent, S. Hill, J. M. North, N. S. Dalal, E. M. Rumberger, D. N. Hendrickson, N. Chakov, and G. Christou, *J. Low Temp. Phys.* **140**, 119 (2005).  
<sup>19</sup>K. Park, T. Baruah, N. Bernstein, and M. R. Pederson, *Phys. Rev. B* **69**, 144426 (2004).  
<sup>20</sup>D. A. Garanin and E. M. Chudnovsky, *Phys. Rev. B* **78**, 174425 (2008).  
<sup>21</sup>A. J. Millis, A. D. Kent, M. P. Sarachik, and Y. Yeshurun, *Phys. Rev. B* **81**, 024423 (2010).  
<sup>22</sup>T. Lis, *Acta Crystallogr., Sect. B: Struct. Sci.* **36**, 2042 (1980).  
<sup>23</sup>Different local values of magnetization may be obtained by a micron-sized Hall bar at different points on the sample due to demagnetization effects arising either from the sample shape or from surface demagnetization effects. Recent superconducting quantum interference device-based studies of Curie-Weiss temperature,  $T_{CW}$ , in  $Mn_{12}$ -ac samples with different aspect ratio (unpublished) show a strong dependence of  $T_{CW}$  on shape. Mean-field theory for a dipolar magnet indicates [see Eq. 21 of Ref. 3] that demagnetization effects enter  $\chi^{-1}$  as an additive correction to the interaction coefficient  $J$ , thus as a shift in the apparent Curie-Weiss temperature,  $T_{CW}$ . To eliminate these effects from our data analysis, we renormalize the theoretical calculations to agree with experimental values in zero transverse field.  
<sup>24</sup>J. R. Friedman and M. Sarachik, *J. Appl. Phys.* **81**, 3978 (1997).  
<sup>25</sup>D. A. Garanin and E. M. Chudnovsky, *Phys. Rev. B* **56**, 11102 (1997).  
<sup>26</sup>J. R. Friedman, *Phys. Rev. B* **57**, 10291 (1998).  
<sup>27</sup>R. J. Elliott, P. Pfeuty, and C. Wood, *Phys. Rev. Lett.* **25**, 443 (1970).  
<sup>28</sup>S. McHugh, R. Jaafar, M. P. Sarachik, Y. Myasoedov, H. Shtrikman, E. Zeldov, R. Bagai, and G. Christou, *Phys. Rev. B* **79**, 052404 (2009).